Synchronization Defect Lines in Media with Complex-Periodic Dynamics (Interfaces, Pulses and Waves in Nonlinear Dissipative Systems : RIMS Project 2000 "Reaction-diffusion systems : theory and applications")

AUTHOR(S):

Kapral, Raymond

数理解析研究所講究録
1191 巻 2001 年 99-103

Synchronization Defect Lines in Media with Complex-Periodic Dynamics

Raymond Kapral
Chemical Physics Theory Group, Department of Chemistry, University of Toronto, Toronto, ON M5S 3H6, Canada

Spiral waves in complex-oscillatory or excitable media contain synchronization defect lines which separate domains of different oscillation phases. The phase changes by multiples of 2π across these defect lines and they arise from the need to reconcile the rotation period of a one-armed spiral wave with the oscillation period of the local dynamics. Synchronization defect lines are analysed and classified. Spatially distributed systems of this type may also exhibit line defect turbulence due to the nucleation, growth and destruction of defect lines. The transitions to line defect turbulence are non-equilibrium phase transitions characterized by power law behavior of order parameters.

I. INTRODUCTION

Along with simple period-1 dynamics, almost all known oscillatory reactions also display complex-periodic, aperiodic or chaotic behavior. [1] A complex-periodic oscillation is characterized by many peaks per full period if viewed as a time series of a single concentration variable and, in a suitably chosen concentration phase space, it corresponds to an orbit which loops several times before it closes onto itself. Period doubled oscillations have period $T_n \approx 2^n T_0$, where T_0 is the period of the orbit which spawned the period-doubling cascade, and have 2^n loops in a phase space representation of the orbit. We consider situations where the local dynamics in a spatially-extended system exhibits such period-doubled temporal patterns.

Complex or chaotic oscillations are quite common and expected to be generic for systems with more than two local scalar fields although little is known about the spatiotemporal dynamics of media with such local oscillations. We show that in most circumstances the basic spatial patterns still exist and, in particular, spiral waves are easily observed; however, new features appear giving rise to qualitative changes in the overall synchronization of the medium.

In Section II we describe synchronization defect lines, which have been observed in numerical simulations [2–7] and experiments [8,9]. The study of synchronization defect lines is continued in Section III gives a classification of defect lines and outlines a complete solution to the classification problem for period-doubled media with period-2^n local dynamics. The role of defect lines in the transition from complex-periodic to chaotic dynamics is considered in Sec. IV. The conclusions are given in Sec. V.

II. SYNCHRONIZATION DEFECT LINES

We examine systems described by a reaction-diffusion equation with a local reaction rate term, $\mathbf{R}(\mathbf{c}(\mathbf{r},t))$. As a specific example of a reaction-diffusion system with complex local dynamics we take $\mathbf{R}(\mathbf{c})$ to be given by the Rössler model [10] with $R_x = -c_y - c_z$, $R_y = c_x + Ac_y$, $R_z = c_x c_z - Cc_z + B$. This system was investigated for C in the interval [2.,6.] with the other parameters fixed at $A = B = 0.2$. We observed that the spatially-distributed system undergoes period-doubling bifurcations. Simulations designed to characterize the period-doubling transitions were performed on a disk-shaped domain ($R = 256, D = 1.6$) with a single spiral wave in the center. [2,4] The spiral wave concentration profile in the period-1 regime was taken as the initial condition and the parameter C was gradually incremented. This system undergoes a first period-doubling bifurcation at $C = C_1^* \approx 3.03$. Within the period-2 domain, the spiral wave acquires a global structure that differs from that in a simple periodic medium. Figure 1 shows the $c_z(\mathbf{r}, t_0)$ concentration field at a single time instant t_0.

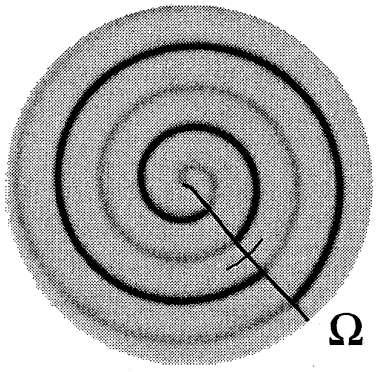

FIG. 1. Spiral wave in the Rössler medium with no-flux boundary conditions and period-2 local dynamics at $C = 3.84$. Concentration field $c_z(\mathbf{r}, t)$ is shown as grey shades. The solid line depicts the Ω curve. Dynamics on the small arc segment that transversally cuts the Ω curve is described below.

The main feature of this spiral wave is the presence of a line, labeled Ω in Fig. 1, which connects the spiral wave core to the boundary. Along this line the pattern is displaced by one wavelength. While the wave propagates, the dislocation line remains stationary. The concentration time series at any two nearby points on opposite sides of this line are shifted in time relative to each other by one period of rotation of the spiral. The passage of a high-amplitude wave maximum through one observation point is synchronized with the passage of a low-amplitude

maximum through the other and vice versa. We call this line a *synchronization defect line.* Two arbitrary states of the spiral wave evolution cannot be transformed into each other by simple rotation of the entire concentration field. After one turn of the spiral the high and low maxima interchange and it is only after two spiral revolutions that the concentration field is restored to its initial value.

Figure 2 shows local orbits calculated at five different points on the arc shown in Fig. 1 with radius $r_0 = 130$ and monotonically increasing θ.

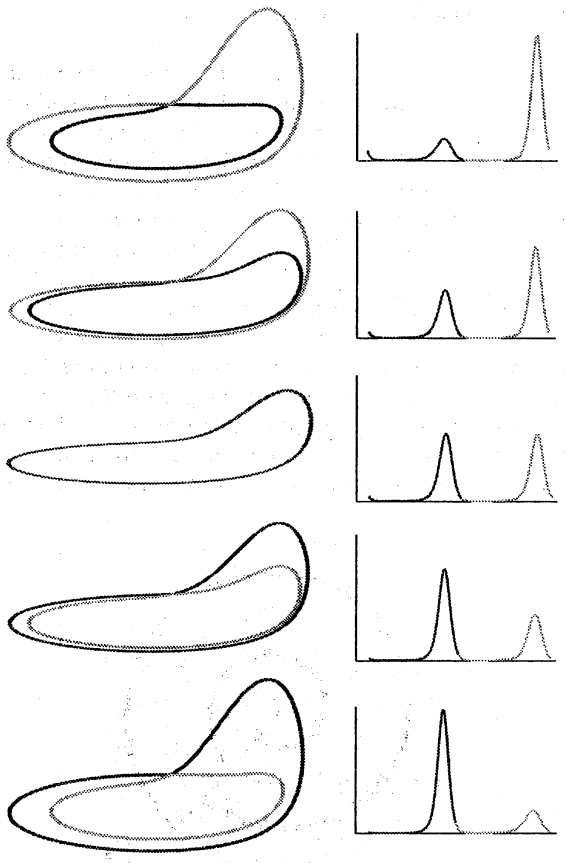

FIG. 2. Loop exchange in local orbits as the Ω curve is crossed. Right column displays the $c_z(\theta, t)$ time series corresponding to the orbits in (c_x, c_y, c_z) phase space shown in the left column.

As one traverses the arc, the larger, outer loop of the local orbit constantly shrinks while the smaller, inner loop grows. At $\theta = \theta_\Omega$, both loops merge and then pass each other exchanging their positions in phase space. As one sees from Fig. 2, at the exchange point $\theta = \theta_\Omega$ not only are the c_z maximum values of two loops equal $(\delta_1 c_z(\theta_\Omega) = 0)$, but the entire loops coincide in phase space and the local oscillation is effectively period-1.

Synchronization defect lines have been observed experimentally in a spatially heterogeneous BZ reaction system consisting of thin (0.7 mm) layer of a Mn-catalyzed BZ reaction mixture with a monolayer of the surfactant-derivative of the ruthenium-bipiridil complex on its top [8]. Synchronization defect lines have also been observed in another set of experiments on the BZ reaction under different conditions by Park and Lee [9].

A. Period-4 synchronization defects

As n for a period 2^n orbit increases one expects the diversity of defects will grow since the total phase shift associated with defect lines increases. As the parameter C is increased a second period-doubling is observed at $C_2^* = 4.075$. The transition to period-4 dynamics results in the doubling of the spiral wavelength, while the wave preserves its one-armed geometry. Therefore, the instantaneous concentration profile of the spiral wave normal to its front exhibits four different maxima corresponding to four different loops of the local orbit. The loops may be numbered according to their position in phase space starting from innermost loop. Then, up to cyclic permutations, the wave maxima follow each other in the order $4 \to 1 \to 3 \to 2$. This is the order in which the loops are visited during one full period of the dynamics. After one spiral rotation the bands exchange according to the permutation $\binom{1234}{3421}$ defined by the order of loop succession. Naturally, it takes four spiral rotations for the pattern to return to itself.

Two types of defect line exist which we denote Ω_1 and Ω_2. As in the case of the prototypical Ω curve, a certain value of the phase shift, expressed in fractions of the full-period phase increment 8π, is associated with crossings of the Ω_1 and Ω_2 curves. Similar to the Ω curve, crossing of Ω_2 leads to a half-period shift which amounts to a 4π phase translation. The specific nature of the half-period time shift is such that it is not possible to determine which oscillation is advanced, since a translation by $T_4/2$ forward is equivalent to a shift by $T_4/2$ backward. This is not the case for the crossing of the Ω_1 line where the oscillation acquires a quarter-period $+2\pi$ or minus quarter-period phase shift $-2\pi \equiv 6\pi$, depending on the direction of crossing.

As in the period-2 medium, the phase discontinuity on the Ω_1 and Ω_2 curves results from loop exchanges. It is convenient to denote the loop exchanges by permutations which specify for every loop with number ℓ of the oscillation pattern on one side of the defect, the loop with number m which is executed by the local dynamics on the other side of the defect at the same time instant. Thus, for the crossings of the Ω_1 curve in opposite directions, different loop exchange permutations are assigned: $\binom{1234}{3421}$ for the $+2\pi$ shift and $\binom{1234}{4312}$ for -2π.

III. CLASSIFICATION OF DEFECT LINES

One can represent the loop exchanges for a particular type of defect line symbolically by a permutation

which, for loop m_i, $i = 1, \ldots n$, of a period-n orbit specifies another loop m_j, $j = 1, \ldots n$, $j \neq i$ into which it transforms under the exchange. Since the phase jump on the Ω curves is always an integer multiple of 2π, to characterize the jump one needs only a coarse-grained description of the orbit with 2π being the minimum detectable quantum of the phase change. At $t = t_0$ let the phase point of the period-n orbit be somewhere on the m_1-th loop, at $t = t_0 + T_n/n$ on the m_2-th loop, and so on (where $m_l \in [1,n]$, $l \in [1,n]$, $m \neq l$) until at $t = t_0 + T_n$ the phase point returns to the m_1-th loop and the pattern $(m_1, m_2, \ldots, m_n)$ repeats. The symbolic string $s = (m_1, \ldots, m_n)$ constructed in this way captures the most significant gross features of the oscillation pattern. An oscillation shifted by 2π forward relative to s is given by the string $(m_2, \ldots, m_n, m_1)$ while the oscillation shifted by 2π backward reads $(m_n, m_1, \ldots, m_{n-1})$. Any phase translation by $\pm 2\pi k$ is represented by one of the n cyclic permutations of the symbolic string s. To find how the crossing of particular line defect affects the phase of the local oscillation one needs to act with the corresponding exchange permutation on a trial symbolic string and compare the result to the initial state. Consider as an example the Ω_2 curve described by the exchange permutation $\binom{1234}{2143}$. Acting with it on the trial state (4132) one finds

$$\binom{1234}{2143}(4132) = (3241),$$

which corresponds to 4π phase shift of the initial state. This result does not depend on the choice of the trial state. Action of the exchange permutation on any of the four different period-4 strings results in another string translated by 4π relative to the initial string. In the general case of period-n dynamics, the exchange permutations correspond to operators which map the set of all possible symbolic strings onto itself. These operators form a group.

To classify all synchronization line defects existing in the period-n medium and find the associated phase shift values, one needs to identify all possible types of loop exchange allowed by the topology of the orbit and select those that correspond to nontrivial phase translations. One needs a means to characterize a period-n orbit topologically.

A general open braid [11] b_n is a topological object which consists of n oriented threads forming a tangle as they run from one end to the other. Each crossing of the threads i and $i+1$ is assigned an elementary braid

One may consider possible loop exchanges for the period-2^n period-doubled orbits and show how these exchanges influence the corresponding patterns of oscillation. A period-2 orbit is represented by the simplest nontrivial braid $\overline{B_2} = \overline{\sigma_1}$ shown in Fig. 3. Consider the first Markov move $\mathcal{M}_1^{(1)}$ which propagates the elementary braid σ_1 by 2π around the braid $\overline{B_2}$ in a direction opposite to the flow.

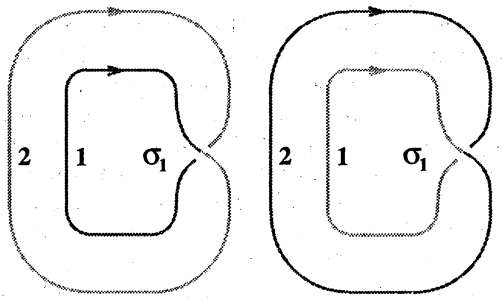

FIG. 3. Propagation of σ_1 around the $\overline{B_2}$ braid results in the exchange of loops.

The superscript in parentheses denotes the power n while the subscript numbers the moves consecutively. Although the braid $\overline{B_2}$ remains unchanged as a result of this move, one finds that the two loops have interchanged their positions. To indicate this the loops of $\overline{B_2}$ are drawn in different line styles in Fig. 3. The left panel shows $\overline{B_2}$ before the application of $\mathcal{M}_1^{(1)}$ and the right panel after. In this way the exchange operators and algebraic relations between them can be established for period-doubled orbits with higher n.

IV. LINE DEFECT TURBULENCE

Thus far we have considered the description and analysis of line defects in systems with period-2 and period-4 dynamics in the period doubling cascade. As C is increased one finds a complex scenario which involves turbulent stages characterized by spontaneous formation, erratic motion and proliferation of synchronization defect lines. To characterize line-defect turbulence quantitatively one needs a means to both visualize the dynamics of the Ω lines and measure their density. To this end scalar fields were defined [6] in the following way: during four consecutive rotations of the spiral wave the values of the $c_z(\mathbf{r})$ concentration maxima $A_i(\mathbf{r}), i = \overline{1,4}$ were collected at every point in the medium and sorted so that $A_1(\mathbf{r}) \leq A_2(\mathbf{r}) \leq A_3(\mathbf{r}) \leq A_4(\mathbf{r})$. The scalar fields are defined as $\xi_1(\mathbf{r}) = A_4(\mathbf{r}) - A_1(\mathbf{r})$ and $\xi_2(\mathbf{r}) = A_4(\mathbf{r}) - A_3(\mathbf{r})$. By construction, $\xi_1(\mathbf{r})$ and $\xi_2(\mathbf{r})$ take on fixed, non-zero values at points in the medium with period-4 dynamics and vanish at points where the loop exchanges occur. Indeed, $\xi_1(\mathbf{r})$ decreases to zero on the Ω_1 curves while $\xi_2(\mathbf{r})$ vanishes on both the Ω_1 and Ω_2 curves. The $\xi_1(\mathbf{r})$ and $\xi_2(\mathbf{r})$ fields allow one both to determine the lengths of the Ω curves and to visualize them. Figure 4, panel (c), shows the $\xi_2(\mathbf{r})$ field at $C = 4.3$ for a medium with periodic boundary conditions supporting a spiral pair. The corresponding phase $\varphi(\mathbf{r}, t_0)$ and $c_z(\mathbf{r}, t_0)$ fields are shown in panels (a) and (b), respectively. The cores of spiral waves, seen as black disks, are connected by a common Ω_1 curve which appears as a wide, nearly straight black line. At this value of C the dynamics in the bulk of the medium (spiral cores, Ω_1 curve, and shock lines

excluded) is given by a period-4 pattern (see Fig. 5(a)). The shock lines, where the spiral waves collide, are seen in panels (c) and (d) as one vertical and two horizontal strips where the grey shades are inhomogeneous. This inhomogeneity in the $\xi_2(\mathbf{r})$ field indicates that the local dynamics on the shock lines is different from that in the bulk. Indeed, the calculations show that the local dynamics on the shock lines at $C = 4.3$ is given by two-banded chaos (see Fig. 5(b)). The chaotic dynamics on the shock lines gives rise to spatially coherent fluctuations of $A_i(\mathbf{r})$ fields seen in Fig. 4(c) as darkly shaded "breathing spots". Sufficiently large fluctuations (like that indicated by the arrow in the figure) may result in the creation of "bubbles" – domains delineated by circular Ω_2 curves (cf. Fig. 4(d)). For $C \leq C_{\Omega_2} = 4.306$, the bubbles are formed with a size smaller than a certain critical value and collapse shortly after birth. As C increases beyond C_{Ω_2}, the bubble nuclei begin to proliferate, forming large domains whose growth is controlled by collisions with spiral cores or other domains

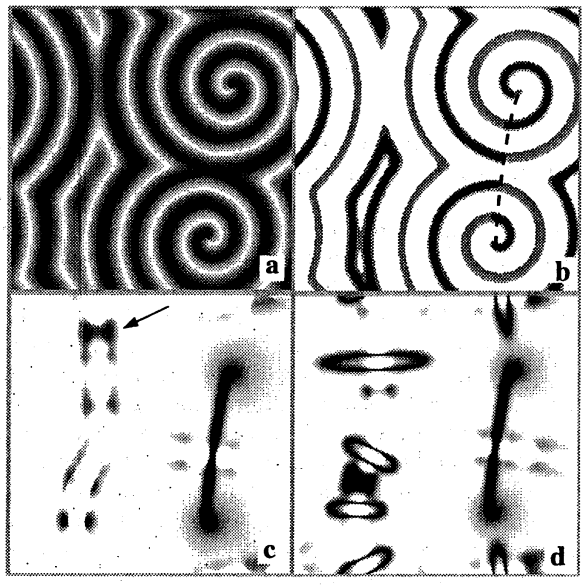

FIG. 4. Representation of defect lines by the $\xi_2(\mathbf{r})$ field for the medium with two spiral waves at $C = 4.30$ (c) and $C = 4.32$ (d). Panels (a) and (b) show, respectively, the $\varphi(\mathbf{r}, t_0)$ and $c_z(\mathbf{r}, t_0)$ fields calculated for the medium in panel (c).

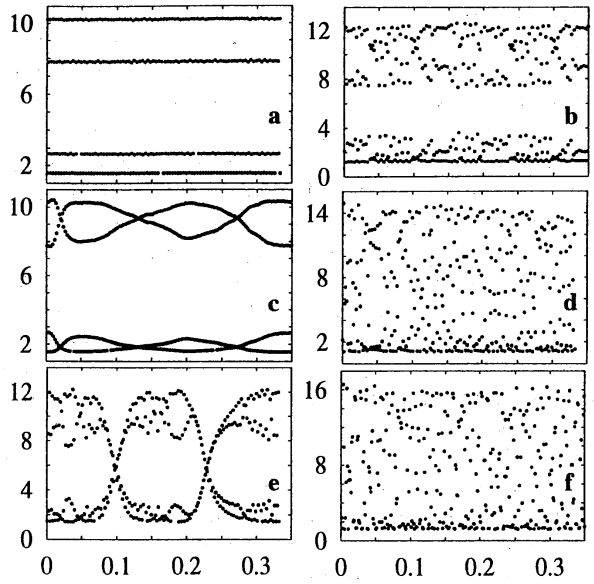

FIG. 5. Time series of the c_z concentration maxima: a,b) $C = 4.30$, c,d) $C = 4.42$ and e,f) $C = 4.7$. Left panels show the local dynamics at a point in the bulk, while the right panels show the dynamics on the shock lines. Time is in units of thousands of spiral revolutions. In panels (c) and (e), respectively, the crossing of the c_z maxima reflect the passages of an Ω_2 or Ω_1 line through the observation point in the medium.

The transition to line-defect turbulence changes the character of the local dynamics observed in the bulk of the medium. As the Ω_2 lines propagate through the medium the associated loop exchanges result in an effective band-merging in the orbits of local trajectories so that they take the form of two-banded chaotic trajectories (cf. Fig. 5(c)). As C increases past $C \approx 4.5$ the local dynamics fails to exhibit a period-4 pattern in the intervals separating line defect passages and shows thick four-banded orbits whose bands grow in width with increasing C. The width of chaotic bands varies from point to point and while in some locations one observes their merging, in others there might be a distinct gap between them. The local dynamics on the shock lines also progresses towards less-structured chaos. At $C = 4.42$ (cf. Fig. 5(d)) it already exhibits one-banded chaos.

From these observations it follows that the evolution of the size and shape of a domain is controlled by the balance of two competing factors: propagation of defect lines along the phase gradient directed to the spiral wave cores which results in line growth, and the tendency of diffusion to eliminate curvature and reduce the length of defect lines.

V. CONCLUSIONS

In this talk an overview of synchronization defect lines in two-dimensional complex-periodic and chaotic media was presented. Stable spiral waves in such systems are

one-armed and, therefore, characterized by a topological charge $n_t = \pm 1$. In one turn of such a spiral wave the local complex-periodic dynamics executes only a fraction of the full oscillation period and the concentration field does not return to its initial state. For example, in the period-2 medium it takes two rotations of the spiral for the concentration field to be restored. This conflict between the spiral rotation period and the period of the local oscillation is reconciled by the presence of a synchronization defect line connecting the wave core to the boundary or to another spiral wave core with opposite topological charge.

Synchronization defects also play an important role in the transition to chaos. In this transition, media supporting spiral waves exhibit line-defect turbulence characterized by proliferation, erratic motion and collision of defect lines. In this regime the dynamics of defects is controlled by two factors: growth along the phase gradient and the tendency of diffusion to reduce their length and curvature. The balance of these factors gives rise to a statistically stationary density of defect lines which varies with the parameters. A power-law form of this variation indicates that the transitions to line-defect turbulence can be considered as non-equilibrium phase transitions.

ACKNOWLEDGEMENTS

This research was supported in part by a grant from the Natural Sciences and Engineering Research Council of Canada.

[1] S. Scott, *Chemical Chaos*, Oxford University Press, New York, (1991).
[2] A. Goryachev and R. Kapral, *Phys. Rev. E*, **54**, 5469, (1997).
[3] A. Goryachev and R. Kapral, Phys. Rev. Lett., **76**, 1619 (1996).
[4] A. Goryachev, H. Chaté, and R. Kapral, *Phys. Rev. Lett.*, **80**, 873, (1998).
[5] A. Goryachev and R. Kapral, Int. J. Bif. Chaos, **9**, 2243 (1999).
[6] A. Goryachev, H. Chaté, and R. Kapral, *Phys. Rev. Lett.*, **83**, 1878, (1999).
[7] A. Goryachev, H. Chaté, and R. Kapral, Int. J. Bif. Chaos, **10**, 1537 (2000).
[8] M. Yoneyama, A. Fujii, and S. Maeda, *J. Am. Chem. Soc.*, **117**, 8188, (1995).
[9] J.-S.Park and K. J. Lee, to be published.
[10] O. E. Rössler, *Z. Naturforsch.*, **31**, 1664, (1976).
[11] J. S. Birman, *Braids, Links and Mapping Class Groups*, Princeton Univ. Press, Princeton (1974).